Published online 7 March 2018

Nucleic Acids Research, 2018, Vol. 46, No. 9 ***4533–4545***
doi: 10.1093/nar/gky173

Human RTEL1 stabilizes long G-overhangs allowing telomerase-dependent over-extension

Rosa M. Porreca[1], Galina Glousker[2], Aya Awad[2], Maria I. Matilla Fernandez[3], Anne Gibaud[1], Christian Naucke[1], Scott B. Cohen[3], Tracy M. Bryan[3], Yehuda Tzfati[2], Irena Draskovic[1,*] and Arturo Londoño-Vallejo[1,*]

[1]Institut Curie, PSL Research University, Sorbonne Universités, CNRS UMR3244 Telomere and cancer lab, 75005 Paris, France, [2]Department of Genetics, The Silberman Institute of Life Science, The Hebrew University of Jerusalem, Safra Campus—Givat Ram, Jerusalem 91904, Israel and [3]Children's Medical Research Institute, University of Sydney, Westmead, NSW 2145, Australia

Received August 02, 2017; Revised February 23, 2018; Editorial Decision February 26, 2018; Accepted March 01, 2018

ABSTRACT

Telomere maintenance protects the cell against genome instability and senescence. Accelerated telomere attrition is a characteristic of premature aging syndromes including Dyskeratosis congenita (DC). Mutations in hRTEL1 are associated with a severe form of DC called Hoyeraal-Hreidarsson syndrome (HHS). HHS patients carry short telomeres and HHS cells display telomere damage. Here we investigated how hRTEL1 contributes to telomere maintenance in human primary as well as tumor cells. Transient depletion of hRTEL1 resulted in rapid telomere shortening only in the context of telomerase-positive cells with very long telomeres and high levels of telomerase. The effect of hRTEL1 on telomere length is telomerase dependent without impacting telomerase biogenesis or targeting of the enzyme to telomeres. Instead, RTEL1 depletion led to a decrease in both G-overhang content and POT1 association with telomeres with limited telomere uncapping. Strikingly, overexpression of POT1 restored telomere length but not the overhang, demonstrating that G-overhang loss is the primary defect caused by RTEL1 depletion. We propose that hRTEL1 contributes to the maintenance of long telomeres by preserving long G-overhangs, thereby facilitating POT1 binding and elongation by telomerase.

INTRODUCTION

Telomeres are specialized nucleoprotein structures that play a critical role in protecting chromosome ends from DNA damage and degradation. Mammalian telomeres consist of repetitive TTAGGG sequences, which terminate in a 3' single-strand G-overhang (1,2). These repetitive sequences are associated with a protein complex, named Shelterin, which specifically binds the canonical telomeric repeats orchestrating the capping of telomeres (3). In human cells, this complex consists of proteins TRF1, TRF2, RAP1, TIN2, TPP1 and POT1, among which TRF1 and TRF2 bind the telomeric double-strand DNA, while POT1 binds specifically the G-overhang (4). This 3' overhang can invade more internal double-stranded repeated tracts to form a loop structure called the T-loop (5,6). In somatic cells, telomere length declines with each cell division, ultimately leading to replicative senescence (7). The majority of cancer cells counteract telomere loss by the expression of telomerase, a ribonucleoprotein complex containing a reverse transcriptase (hTERT) and an RNA template (hTR), which adds telomeric repeats to the 3' end of the telomeric overhang (7,8).

RTEL1, regulator of telomere elongation helicase 1, was discovered in mice as an essential factor for telomere length maintenance and genomic stability (9). While *Rtel1* deletion was embryonic lethal, mouse embryonic stem cells (mESCs) lacking *Rtel1* displayed chromosome aberrations and telomeric loss (9). In addition, these cells were hypersensitive to interstrand crosslinking agents and showed an increased rate of sister chromatid exchanges (SCEs), suggesting a role of RTEL1 in resolving recombination intermediates (10). Consistently, chromosomal and telomeric aberrations were also observed in mouse embryonic fibroblasts (MEFs) deleted for *Rtel1*, leading to the hypothesis that telomere instability in the absence of Rtel1 originates from both replication fork stalling due to unresolved G-quadruplex structures and inappropriate resolution of T-loops, introducing telomere deletions and accumulation of T-circles (11,12). In all, mouse Rtel1 appears to be required genome-wide for replication, recombination and DNA repair, and specifically at telomeres for the disassembly of G-

*To whom correspondence should be addressed. Tel: +33 156246611; Fax: +33 156246674; Email: Arturo.Londono@curie.fr
Correspondence may also be addressed to Irena Draskovic. Email: Draskovic@curie.fr

quadruplexes and T-loops, allowing correct replication of chromosome ends.

In humans, germline mutations in RTEL1 have been found in patients with Hoyeraal-Hreidarsson syndrome (HHS), a severe form of dyskeratosis congenita, characterized by accelerated telomere shortening (13–17). Cell lines obtained from patients carrying RTEL1 mutations displayed growth defects in culture, short telomeres, short telomeric overhang (18) and telomeric aberrations (15,16). Telomere phenotypes associated with a specific mutation in RTEL1 can be phenocopied by a point mutation in the TRFH domain of TRF2, thus providing evidence that these two proteins interact (19). Although these findings strongly suggest a direct link between RTEL1 and telomere-related diseases, the precise role of human RTEL1 in telomere maintenance remains to be determined.

In this work we have characterized the effects of RTEL1 knockdown on human telomere maintenance. We found that RTEL1 is required for telomere maintenance in telomerase-positive cells with long telomeres in a telomerase-dependent way. In RTEL1-depleted cells, we observed a reduction of G-overhang content and of telomeric POT1. Unexpectedly, we found that the loss of G-rich overhangs was a primary defect in RTEL1-depleted cells and not the consequence of the reduction of POT1 at telomeres since overexpression of the latter only rescued the shortening phenotype. In all, our results demonstrate that RTEL1 promotes the stability of the G-rich telomeric overhang/POT1 complex thus allowing telomerase to overextend long telomeres.

MATERIALS AND METHODS

Cell lines

HCA2 cells are primary human foreskin fibroblast obtained from O.M. Pereira-Smith, Baylor College (20). HT1080 human fibrosarcoma cell line and its derivative HT1080-ST (stably overexpressing exogenous hTERT and hTR) were a gift from G. Cristofari and J. Lingner (21). TCL1301 is a T-cell leukemia cell line with naturally high telomerase activity and consequently long telomeres (a gift from T. von Zglinicki). U2OS is an osteosarcoma cell line maintaining telomeres by ALT. U2OS-ST (a gift from N. Arnoult and A. Decottignies) contains ectopically expressed telomerase and therefore maintains telomeres by ALT and by telomerase. HeLa I was a gift from S. Bacchetti. Muntjac-hTERT is a fibroblast cell line from the female Indian muntjac deer exogenously expressing hTERT with six diploid chromosomes easily distinguishable from human (a gift from J. Shay).

All cell lines were cultured in Dulbecco's Modified Eagle's Medium (Gibco) supplemented with 10% heat-inactivated fetal calf serum (Bio-West), 5 mM sodium pyruvate and non-essential amino acids (Gibco). Cell cultures were cultivated at 37°C with 5% CO_2.

Transfections with siRNAs and plasmids

One million cells were transfected with 10 μM siRNA (siContr, 5′-CGUACGCGGAAUACUUCGA-3′; siRTEL1#1, 5′-GCCUGUGUGUGGAGUAUGA-3′; siRTEL1#2, 5′-GACCAUCAGUGCUUACUAU-3′, all from Eurogentec) using cell line specific Nucleofection Kits (Lonza). Following the transfection cells were collected after 72 h for telomerase+ cell lines and after 120 h for primary and ALT cells. The plasmids pEGFP-C1::POT1 and pEGFP-C1::NLS_{SV40}-OB_{POT1} were described (22), pEGFP-C1 (CloneTech) was used for GFP expression.

For genome-editing approaches targeting the *hTERT* gene, HT1080-ST cells were transfected with hTERT CRISPR/Cas9 KO Plasmid (h) (Santa Cruz, sc-400316) or a control CRISPR/Cas9 Plasmid (Santa Cruz, sc-418922). The CRISPR/Cas9 KO Plasmid is a mixture targeting three different exons of the *hTERT* gene. Both TERT- and control-CRISPR plasmids express a GFP, which allows enrichment of highly transfected cells by cell sorting. Twenty-four hours post-transfection, single GFP-positive cells were sorted into 96-well plates using the FACSAria flow cytometer. Thirty clones for hTERT and 23 clones for control plasmid were expanded and cultured for 20 PDs before screening for telomerase activity. Among them 12 hTERT clones were negative for telomerase activity.

Western blot

Cells were pelleted, washed twice in phosphate-buffered saline (PBS) 1×, incubated in RIPA buffer (Tri–HCl 50 mM, pH 7.9; NaCl 120 mM; ethylenediaminetetraacetic acid (EDTA) 1 mM; Nonidet P-40 0.5%; 1× Halt phosphatase inhibitor, Thermo scientific; Complete protease inhibitor cocktail, EDTA-free, Roche) for 30 min on ice and spun for 30 min at 16 000 *g* at 4°C. A total of 20 μg of protein lysates were separated on 4–12% Bis-Tris gels (Invitrogen) and transferred onto a nitrocellulose membrane. Rabbit anti-RTEL1 (produced in-house, 1:50 000 (16)), rabbit anti-POT1 (Epitomics, 1:1000), and mouse anti-GFP (ab290, 1:1000) antibodies were diluted in PBST (Phosphate buffered saline 1×, Life technologies; 0.1% Tween-20, Sigma-Aldrich) with 5% non-fat milk. Following incubations with HRP-coupled secondary antibodies signals were visualized using ECL II kit (Pierce) and Fujifilm LAS-3000 imager. Actin antibody directly coupled to HRP was used for normalization (Santa Cruz, sc-10731).

Metaphase preparation, Q-FISH and CO-FISH

For metaphase preparation, cells were incubated for 90 min with 10 ng/ml colcemid (Gibco). Hypotonic shock was achieved at 37°C under cell line specific conditions: in sodium citrate buffer, 8 g/l, for HT1080 and HT1080-ST (25 min), for U2OS and U2OS-ST (12 min), for HCA2 (30 min), for HeLa I (40 min), in 75 mM potassium chloride for TCL1301 (15 min) and Muntjac-hTERT (20 min). Cells were fixed in ethanol/acetic acid solution (3:1, v/v) and washed three times in this fixing reagent. For normalization of hybridization efficiencies between experimental conditions within the same experiment, some metaphases from the unique Muntjac-hTERT metaphase preparation were mixed into every human metaphase preparation analyzed (23). Metaphase spreads were obtained by dropping suspensions of fixed cells onto clean superfrost slides and dried overnight. Q-FISH and CO-FISH procedures were carried out as described, using a Cy3-O-O-$(CCCTAA)_3$ PNA probe

(TelC PNA, Panagene), and consequently for CO-FISH also a custom made FAM-labeled LNA G-rich telomeric probe (Exiqon) (24). See also Supplementary Material and Methods. Statistical analyses were done using the Wilcoxon rank-sum test.

Immunofluorescence

For detection of RTEL1 at telomeres cells seeded on slides were fixed following a pre-extraction step. After permeabilization nuclei were stained with the anti-RTEL1 antibody (in-house, 1/1000), secondary donkey anti-rabbit Alexa 488 antibody (Invitrogen, 1/400), post-fixed 10 min and hybridized with a TelC PNA probe (Panagene). Following hybridization washes slides were mounted in Vectashield with 0.1 μg 4',6-diamidino-2-phenylindole (DAPI). Image acquisition and analysis were performed at the PICT-IBiSA Imaging Facility using a Nikon 3D microscope. Sixteen stacks, 0.2 μm each, were acquired, deconvolved and average projections were analyzed for the RTEL1 colocalization with telomeres. Colocalization events were individually verified in 3D to exclude the possibility that the overlap is due to the projection.

qPCR-TRAP assay

Whole cell CHAPs extracts corresponding to 1000 cells were analyzed for the telomerase activity using the semi-quantitative polymerase chain reaction (PCR)-based telomeric repeat amplification protocol (TRAP) assay as described (25). See also Supplementary Material and Methods.

Teloblot

Genomic DNA was extracted using the Qiagen DNeasy Kit (Qiagen) according to the manufacturer's instructions. A total of 5 μg of DNA was digested overnight with HinfI and RsaI (40 U each). The digested DNA was resolved on a 1% SeaKem Gold agarose gel (Lonza) in 0.5×Tris/Borate/EDTA (TBE) buffer, using a CHEF electrophoresis chamber (BioRad). Electrophoresis was conducted with initial switch time 0.2 s and final switch time 13 s at 6 V/cm for 15 h. The gel was blotted onto a positively charged Biodyne B nylon membrane (Pall, VWR) and hybridized at 42°C in 6 × saline-sodium citrate buffer (SSC), 0.01% sodium dodecyl sulphate (SDS) with 20 pmol of digoxigenin (DIG)-labeled telomeric C-rich oligonucleotide $TAA(CCCTAA)_4$ prepared using the 3′ end labeling kit (Roche, 03353575910). Following hybridization washes (twice 5 min in 2 × SSC, 0.01% SDS and once 2 min in 0.1 × SSC, 0.01% SDS) the signal was revealed using the anti-DIG-alkaline phosphatase antibodies (Roche, 11093274910) and CDP-Star (Roche) following the manufacturer's instructions. Images were obtained using the Luminescent image analyzer LAS-4000 mini (GE Healthcare) and analyzed using the Telometric 1.2 software.

Meta-TIF assay

The meta-TIF assay for detection of telomere-induced foci (TIF) in metaphase spreads was performed as described (26). See also Supplementary Data.

Chromatin immunoprecipitation (ChIP)

Cells were fixed using 1% formaldehyde (Thermo Scientific, 28908) for 10 min at 37°C and sonicated chromatin was prepared as described in Supplementary Data. Chromatin containing 20 μg DNA was diluted 10 times in ChIP dilution buffer (20 mM Tris–HCl pH 8, 150 mM KCl, 2 mM EDTA pH 8, 1% Triton X-100, 0.1% SDS) and after pre-clearing with Dynabeads (Invitrogen) incubated overnight with 2 μg of antibody (listed in Supplementary Table S1), with the exception of anti-hTERT for which we have used 40 μg, in a total volume of 1 ml. Protein complexes were recovered following a 2 h incubation with Dynabeads and the following washing steps: three times for 10 min in ChIP dilution buffer and twice, 5 min each, in TE (10 mM Tris pH8, 1 mM EDTA). ChIPed material was eluted using 0.1 M $NaHCO_3$, 1% SDS and decrosslinked in the presence of 150 mM NaCl over night at 65°C. DNA was submitted to RNase and proteinase K digestion and purified using a phen–chloroform extraction. Purified DNA was denatured in 0.2 M NaOH by heating at 100°C for 10 min and spotted onto a positively charged Biodyne B nylon membrane (Pall, VWR). Membranes were baked for 15 min at 100°C and UV-crosslinked (Stratalinker, 1800 kJ). Blots were hybridized and detected for telomeric signals as described above for Teloblot. Images were quantified using the Multi Gauge software.

In-gel G-overhang assay

In-gel G-overhang assay was performed as described (27). Following electrophoresis, the gel was dried down under vacuum for 1 h at room temperature and then for 1 h at 50°C, pre-hybridized at 50°C for 1 h in Church mix (0.5 M Na_2HPO_4 pH 7.2, 1 mM EDTA, 7% SDS and 1% bovine serum albumin) and hybridized overnight at 50°C with 5′ radioactively-labeled $(AACCCT)_3$ oligonucleotide. After hybridization, the gel was washed three times with 4 × SSC at room temperature and once with 4 × SSC at 40°C (30 min each wash), and exposed to film or PhosphoImager. Following G-overhang hybridization, gel was denatured by incubation in 0.5 M NaOH and 1.5 M NaCl for 30 min, neutralized in 3 M NaCl and 0.5 M Tris–HCl pH 7.0 twice for 15 min, rinsed with H_2O, prehybridized, hybridized and washed as previously. To determine the relative overhang signal, the signal intensity for each lane was determined before and after denaturation using Image J software. The overhang signal was divided by the signal after denaturation and normalized to the control (set to 1).

Statistical analyses

Statistical analysis was performed using GraphPad Prism 7.0. The P-values < 0.05 were considered statistically significant.

RESULTS

Human RTEL1 is required for telomere length maintenance in telomerase-positive cells with very long telomeres

To analyze the involvement of RTEL1 in telomere maintenance in human cells, we induced siRNA-mediated deple-

tion of the protein in telomerase-negative primary fibroblasts as well as in a panel of telomerase-positive cancer cell lines and examined their telomere lengths. For the telomere length analysis, we used an elaborated version of telomeric quantitative (Q-) FISH analysis, in which metaphase preparations include chromosomes of defined telomere length from a different species (Indian Muntjac). These chromosomes are easily distinguishable from human chromosomes, and facilitate normalization of the FISH signal within and across slides (Figure 1A, see also 'Materials and Methods' section). Acute depletion of RTEL1 resulted in telomere shortening exclusively in cell lines with long telomeres, such as the T-cell leukemia 1301 and cancer cell lines HT1080 and U20S with exogenously added telomerase (so-called supertelomerase -ST- cell lines) (Figure 1B–D). We did not observe any impact of RTEL depletion on telomere lengths in telomerase+ cell lines with short telomeres such as HT1080 and HeLa (Supplementary Figure S1A–C). In telomerase-negative cells with either normal size telomeres (primary HCA2) or long telomeres (U2OS), depletion of RTEL1 by siRNA did not induce telomere shortening (Supplementary Figure S1A–C), suggesting that, in the absence of telomerase, RTEL1 is dispensable for telomere maintenance regardless of telomere length. Collectively, our data indicate that human RTEL1 is a positive regulator of telomere length in telomerase-positive cancer cell lines with long telomeres. Of note, its positive effect on telomere length appears to be directly correlated with the level of telomerase activity detected in *in vitro* assays (Figure 1D and E).

Analysis of single telomere lengths in HT1080-ST cells indicate that the shortening following RTEL1 depletion impacts all telomeres, shifting the entire length distribution to the left (Supplementary Figure S2A and B) without adding length heterogeneity. Repeated depletion of RTEL1 induces cell death and senescence (Supplementary Figure S3A, B and D), an observation supporting the idea that RTEL1 is an essential gene in humans. Therefore, assessments of RTEL1 phenotypes were limited to short-term depletion (72 h for telomerase+ and 120 h for telomerase− cell lines) corresponding to about three population doublings. At 72 h a slight accumulation of cells in G2 was observed in HT1080-ST (Supplementary Figure S3C).

Although T-loop excision has been proposed to be a major mechanism of telomere loss in Rtel1-deficient mouse cells (12), the telomere shortening observed upon RTEL1 depletion in HT1080-ST cells was not associated with either abrupt telomere loss (Supplementary Figure S4A), telomere fragility (Supplementary Figure S4B) or increased T-circle formation (Supplementary Figure S4C), despite the increased levels of recombination, both at telomeres and genome-wide (Supplementary Figure S4D and E). This increased recombination at telomeres, a hallmark of ALT (Alternative Lengthening of Telomeres) activity (28), was not associated with an increase in the production of telomeric C-circles (Supplementary Figure S5), considered the most specific hallmark of ALT (29).

Collectively, transient depletion of RTEL1 gives no observable telomeric phenotype in most human cell lines. However, in a particular context of high telomerase activity and long telomeres, telomere shortening (8–15%) and an increase in T-SCEs (2-fold) are observed. Interestingly, only under the latter conditions RTEL1 is more frequently associated with telomeres, as detected by immunofluorescence (Supplementary Figure S6A and B). While across human cell lines nuclear RTEL1 protein mostly accumulates in discrete foci associated with nucleoli, as previously published (30), it also localizes to individual telomeres in a subpopulation of cells (Supplementary Figure S6A), an association more frequently observed in HT1080-ST (Supplementary Figure S6B).

RTEL1 regulates telomere length through telomerase

In mouse *Rtel1*-/- ESCs, telomeres are stably maintained at a shorter (albeit still long) length, suggesting that hyperelongation by telomerase requires RTEL1 (10). Since we observed telomere shortening upon RTEL1 depletion only in cells with long telomeres and high levels of telomerase, we explored the possibility that in these cells hRTEL1 is required for the elongation of telomeres in a telomerase-dependent manner. After targeting the inactivation of *hTERT* gene using CRISPR/Cas9-mediated genome editing in HT1080-ST cells, we screened several clones for telomerase activity (Figure 2A), using semi-qPCR-based telomeric repeat amplification protocol (qPCR-TRAP). We selected a control clone (C18) and an hTERT CRISPR clone (T25), which based on our analyses presented no TRAP activity (Figure 2B) and showed almost no telomere shortening compared to the parental cell line by terminal restriction fragment analysis (Figure 2C). Then, RTEL1 depletion was induced in both C18 and T25 clones (Figure 2D), followed by telomeric Q-FISH analysis, which revealed telomere shortening only in the control C18 RTEL1-depleted cells (Figure 2E). Indeed, T25 RTEL1-depleted cells exhibited no change in telomere length compared to the same cells transfected with the siRNA control thus confirming that regulation of telomere length maintenance by RTEL1 is telomerase dependent.

RTEL1 is not required for telomerase biogenesis or recruitment of TERT to telomeres

In order to understand the mechanism by which RTEL1 controls telomere length through telomerase, we explored the possibilities that hRTEL1 is required either for telomerase biogenesis or for telomerase recruitment to telomeres. Using immuno-RNA FISH, we checked if depletion of RTEL1 affects the localization of hTR in Cajal bodies, where telomerase complex maturation is deemed to occur (31). We observed no change in the frequency of colocalizations of hTR and Coilin, a major component of Cajal bodies, upon depletion of RTEL1 in HT1080-ST cells (Supplementary Figure S7A and B). Next, we examined the capability of RTEL1-depleted cells to assemble an active telomerase complex using the qPCR-TRAP protocol. Depletion of RTEL1 had no significant effect on the TRAP activity detected in total cell extracts (Supplementary Figure S7C). Next, we evaluated the capacity of telomerase recruitment to telomeres upon depletion of RTEL1 by carrying out a chromatin immunoprecipitation (ChIP) experiment using specific antibodies against hTERT (32,33). The association of hTERT with telomeres was not decreased

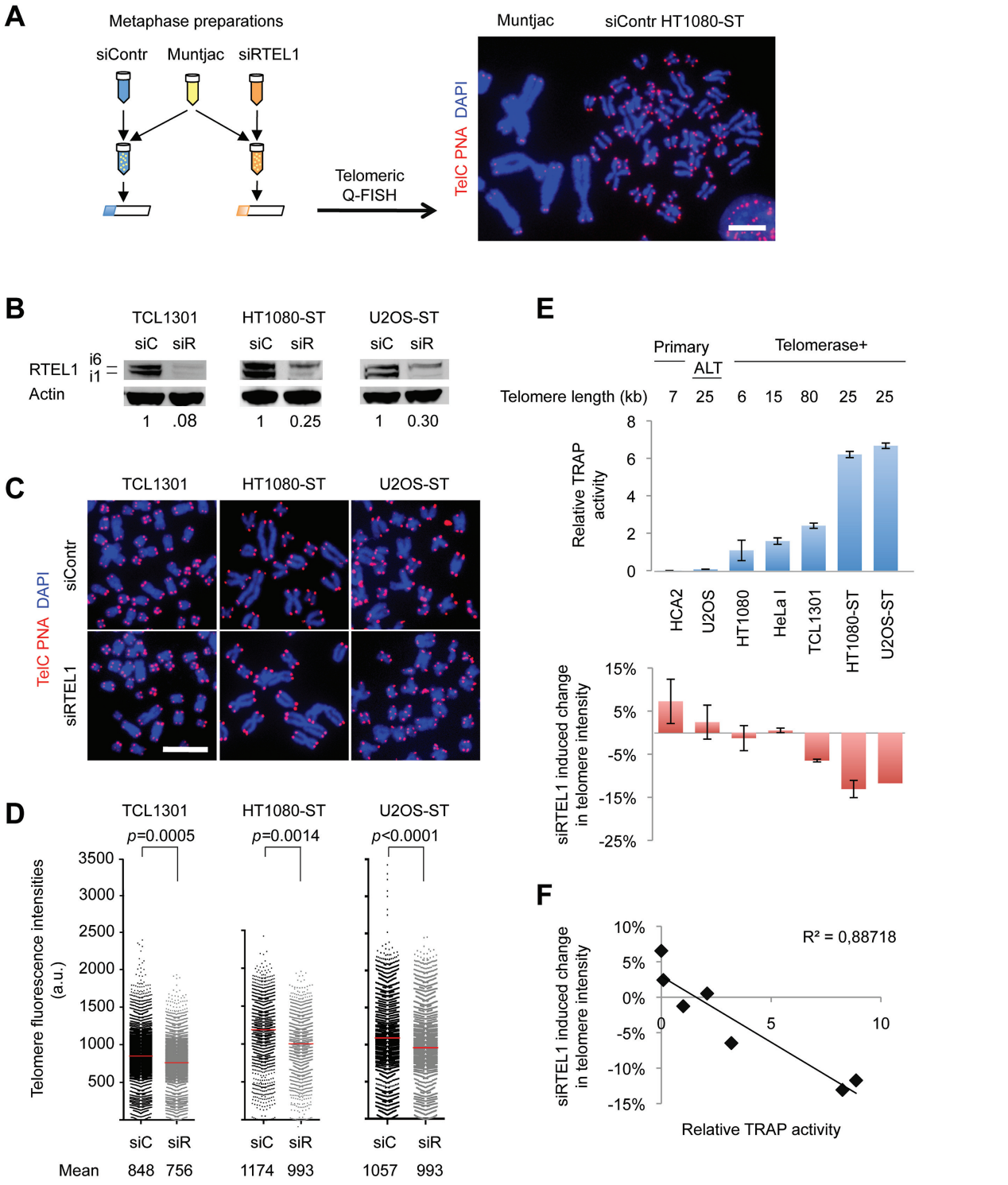

Figure 1. Depletion of RTEL1 induces telomere shortening in telomerase-positive cells with long telomeres. (**A**) hTERT-immortalized Muntjac metaphases from the same preparation were mixed with every metaphase preparation from human cells for normalization of hybridization efficiencies in telomeric quantitative (Q-) FISH. A representative image showing Muntjac and HT1080-ST chromosomes labeled with TelC PNA probe in red and counterstained with DAPI. Scale bar, 10 μm. (**B**) Western blot showing depletion of RTEL1 in TCL1301, HT1080-ST and U2OS-ST following 72-h transfection with siRTEL1. The level of depletion is estimated with regard to the levels detected in siControl-treated cells after actin normalization. (**C**) Representative metaphases of TCL1301, HT1080-ST and U2OS-ST cells transfected with siControl or siRTEL1 after telomeric Q-FISH as described in A. Scale bar, 10 μm. (**D**) Quantification of telomere intensities by Q-FISH after transfection with siControl (siC) and siRTEL1#1 (siR). $n = 30$ metaphases. *P*-values, Wilcoxon rank-sum test. Mean telomere intensities are indicated. (**E**) Mean telomere intensity changes measured by Q-FISH upon RTEL1 depletion in a panel of cell lines including primary, ALT and telomerase-positive cells expressing different levels of telomerase activities as determined by qPCR-TRAP in an *in vitro* assay using protein extracts from 1000 cells. Mean telomere lengths (in kb) were estimated from Southern blots. (**F**) Correlation of data presented in E. A strong negative correlation was observed between the level of TRAP activity and mean telomere intensity change upon siRTEL1.

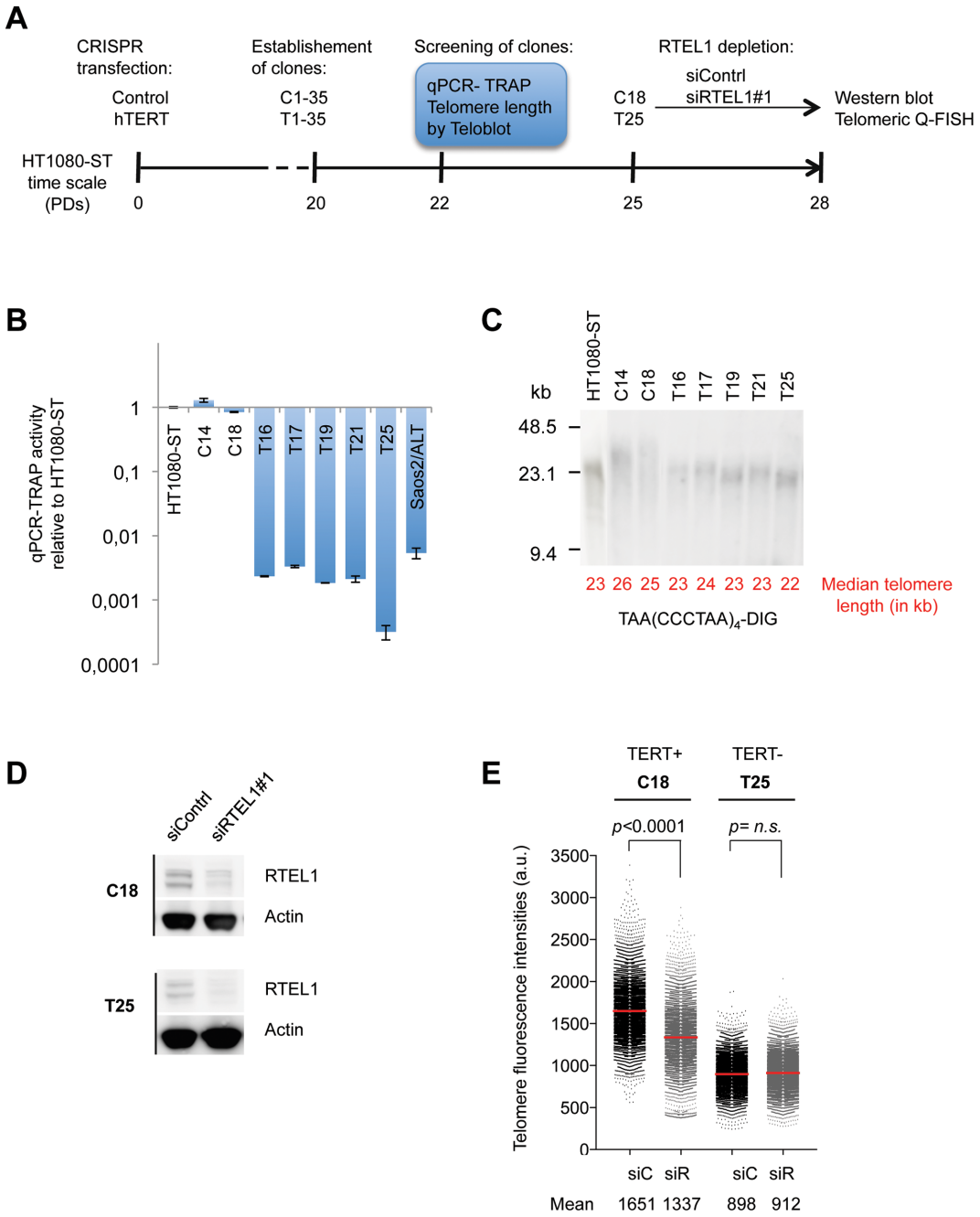

Figure 2. RTEL1 impact on telomere length is telomerase dependent. (**A**) Schematic representation of experimental timeline aimed at testing the role of telomerase in RTEL1-dependent telomere length regulation. HT1080-ST cells were transfected with hTERT-CRISPR/cas9 vectors or control vectors and GFP-positive clones were isolated immediately post-transfection (PD 20). Clones were analyzed for telomerase activity (TRAP) and telomere length (Southern blot) and then chosen clones were transfected with RTEL1 or control siRNA and telomeres measured by Q-FISH. (**B**) Levels of telomerase activity in selected CRISPR/Cas9 clones (C, control and T, targeting TERT), compared to the parental cell line HT1080-ST. Saos2/ALT is a control cell line with no telomerase activity. (**C**) Telomere length analysis by pulse field electrophoresis and blotting with a telomeric C-rich DIG-labeled probe in selected CRISPR/Cas9 clones (C, control and T, targeting TERT) compared to the parental cell line HT1080-ST. Median telomere lengths calculated by the Telometric software are indicated. (**D**) Western blot demonstrating the efficiency of RTEL1 depletion after siRNA in both TERT+ (C18) and TERT− (T25) clones. (**E**) Depletion of RTEL1 leads to telomere length decrease in the TERT+ clone but not in the TERT− clone. Quantification of telomere intensities by Q-FISH after transfection with siControl (siC) and siRTEL1#1 (siR) in clone control C18 and hTERT clone T25. n = at least 40 metaphases. P-values, Wilcoxon rank-sum test. Mean telomere intensities are indicated.

in RTEL1 depleted cells (Supplementary Figure S7D and E); instead, we observed a consistent increased association of hTERT with telomeres, indicating that the recruitment of telomerase to telomeres does not require RTEL1. Our data therefore suggest that while telomerase is being efficiently recruited to telomeres in the absence of RTEL1, the enzyme may not work efficiently on its substrate. We next tested whether combining the RTEL1 depletion with BIBR1532, a telomerase inhibitor that affects telomerase processivity (34) (Supplementary Figure S7F), would have an additive effect. Telomeres of HT1080-ST cells cultured in the presence of the BIBR1532 inhibitor for 40 days showed a mild reduction in mean telomere length by Q-FISH (Supplementary Figure S7G). When combined with a short-term RTEL1 depletion, the level of telomere shortening remained similar to that of RTEL1 depletion alone, suggesting the absence of an additive effect (Supplementary Figure S7G). From these experiments, we conclude that RTEL1 is not required for the biogenesis of telomerase or its targeting to telomeres in HT1080-ST cells. In contrast, RTEL1 is required for efficient telomere elongation by telomerase, either by favoring the interaction between the enzyme with its substrate or by improving its processivity.

RTEL1 is required for the stability of the G-overhang

Since our ChIP experiments showed no impediment to telomerase association with telomeres, we explored the possibility that 3′ G-overhangs, the telomerase substrate, were somehow not suitable for elongation. Using an in-gel hybridization assay, we first analyzed the G-rich single stranded content of telomeres in untreated HT1080 and HT1080-ST cells. Interestingly, in HT1080-ST cells the signal appeared to be much stronger than in the parental HT1080 cells, suggesting that overhangs are over-elongated in the former (Figure 3A). This conclusion is supported by Exonuclease I digestions of the same material, which confirmed that the contribution of replication intermediates to the overall signal is limited in the HT1080-ST cells (Figure 3A). We next quantified the G-overhang content in HT1080-ST cells depleted for RTEL1 and found that the relative amounts of G-overhangs was reduced to 60–70% in RTEL1-depleted cells (Figure 3B–D) in comparison to control cells. A great proportion of the remaining signal after RTEL1 depletion was still sensitive to ExoI digestion, indicating no increase in the accumulation of interstitial single-stranded G-rich sequences, an observation in agreement with the limited impact on telomere replication we observe after RTEL1 depletion. In contrast, no loss of G-overhangs was observed in telomerase+ cells with short telomeres (HT1080) or primary cells HCA2 (Supplementary Figure S8B–D), consistent with the fact that none of these cell lines displayed telomere shortening upon RTEL1 depletion. These observations indicate that RTEL1 is required for the stability of long G-overhangs in cells with long telomeres and high telomerase activity but not in cells with short overhangs and short telomeres, independently of their telomerase status.

RTEL1 is required for telomere protection

None of the human cell types in which we induced RTEL1 depletion showed any signs of overt telomere replication stress, including telomere fragility or sudden telomere loss (Supplementary Figure S4, not shown). However, depletion of RTEL1 appeared to lead to partial telomere deprotection as suggested by limited accumulation of γ-H2AX at chromosome ends in Meta-TIF assays (26) (Figure 4A and B). We hypothesized that this partial deprotection was somehow connected to the observed G-overhang loss and that both manifestations could be secondary to some alteration in Shelterin composition at telomeres. Indeed, it has been shown that POT1 (4) or TRF2 (35,36) dysfunctions cause both telomere deprotection and G-overhang degradation. We therefore probed by ChIP the level of telomere association of TRF1, TRF2 and POT1, the three DNA-binding components of Shelterin. Interestingly, these experiments consistently revealed a reduction in the amount of POT1 at telomeres, while showing that the levels of telomere-associated TRF1 and TRF2 were not significantly affected (Figure 4C–F). This decrease in POT1 at telomeres was not observed in the parental HT1080 cells depleted for RTEL1 (Supplementary Figure S9A–C), in agreement with the absence of impact of RTEL1 depletion on telomere length or G-overhang content in these cells.

Telomere length, but not the G-overhang, is restored in RTEL1-depleted cells by the ectopic expression of full length POT1 or its DNA binding domain

Since POT1 is directly involved in the protection of the G-overhang, we surmised that the G-overhang loss was the consequence of POT1 depletion at telomeres in RTEL1-deficient cells. To test this hypothesis, we over-expressed an exogenous version of POT1, fused to GFP (22), in HT1080-ST cells depleted for RTEL1 and measured its effect on both G-overhang content and telomere lengths (Figure 5A and B). In addition, we analyzed the effect of the C-terminal deletion of POT1 reducing POT1 only to its DNA-binding OB-folds. The expression of the fusion proteins was confirmed by western blotting (Figure 5C). Telomeric Q-FISH analysis revealed that GFP-POT1 expression and OB-folds alone were able to fully rescue the telomere shortening phenotype in RTEL1-depleted cells (Figure 5D and E; Supplementary Figure S10). Unexpectedly, the expression of POT1 constructs was not able to rescue the DNA damage at telomeres (meta-TIF assay, Figure 5A) nor the overhang loss (Figure 5G).

These experiments allow us to conclude that the primary defect induced at telomeres upon RTEL1 depletion is the loss of the telomeric overhang in cells bearing long telomeres with high-telomerase expression.

DISCUSSION

Point mutations in RTEL1 have been associated with the HHS, a severe form of Dyskeratosis congenita in which accelerated telomere shortening is a major manifestation. While mouse models have been instrumental in characterizing the major activities of the protein at telomeres,

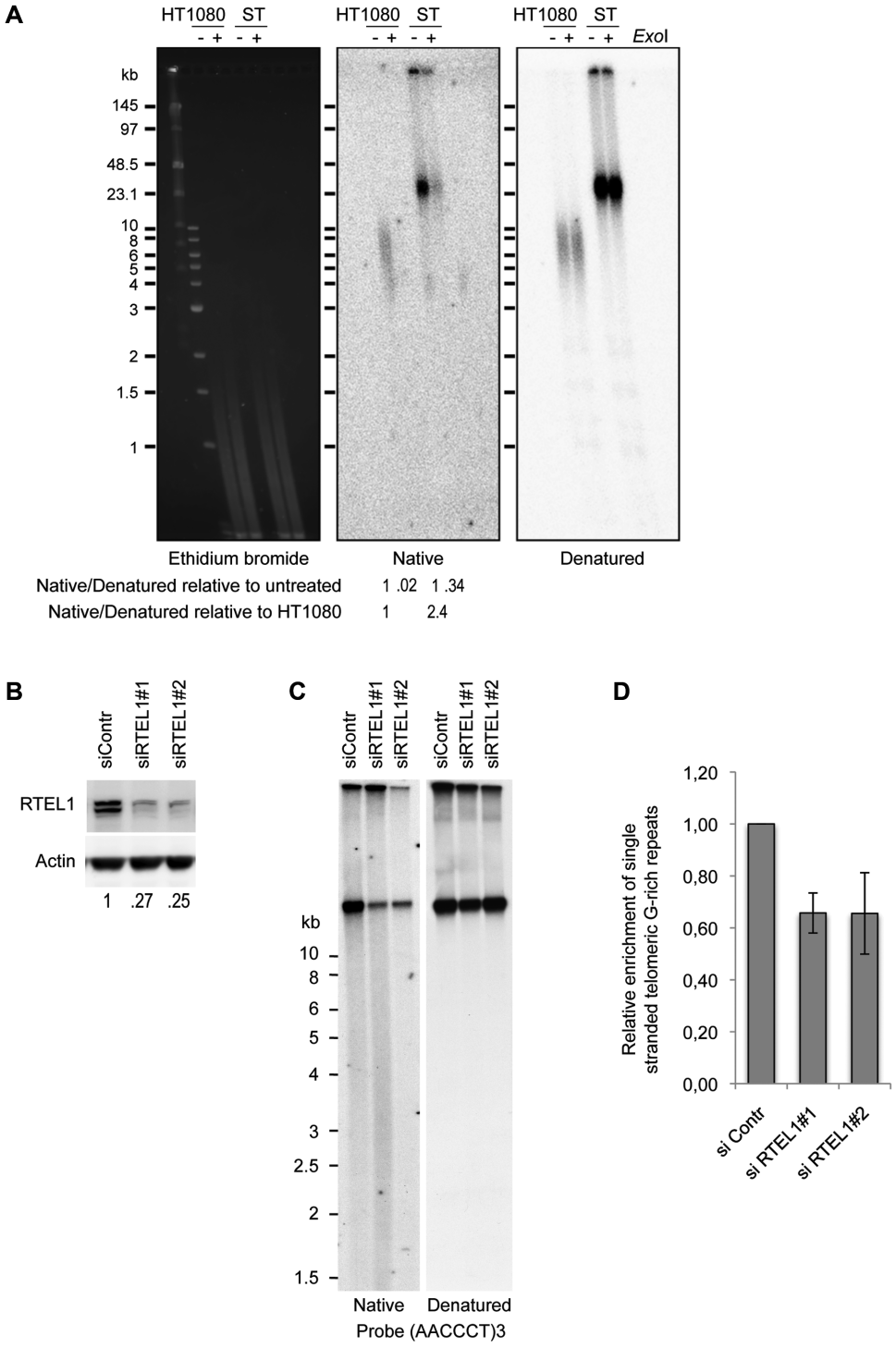

Figure 3. HT1080-ST telomeres have extended overhangs that shorten when RTEL1 is depleted. (**A**) Terminal restriction fragment analysis of genomic DNA (2 μg) by pulsed field electrophoresis from HT1080-ST and HT1080 cells. Panels correspond to an ethidium bromide-stained agarose gel, a native gel to visualize overhangs and a denatured gel to visualize telomeres. Native and denatured gels were probed with a radioactively labeled telomeric C-rich DNA probe. All the panels are from the same experiment and include samples with and without ExoI digestion. (**B**) Depletion of RTEL1 by western blot. (**C**) In-gel hybridization under native condition using a radioactively labeled telomeric C-rich probe for detection of telomeric single stranded G-rich repeats using 3.25 μg of digested genomic DNA. After denaturation, the gel was re-hybridized using the same probe to detect the total amount of telomeric G-rich repeats. (**D**) Quantification of C. The amounts of single stranded telomeric G-rich repeats were normalized with total telomeric G-rich repeats and are represented relative to siControl. Data are represented as mean ($n = 3$) ± SEM.

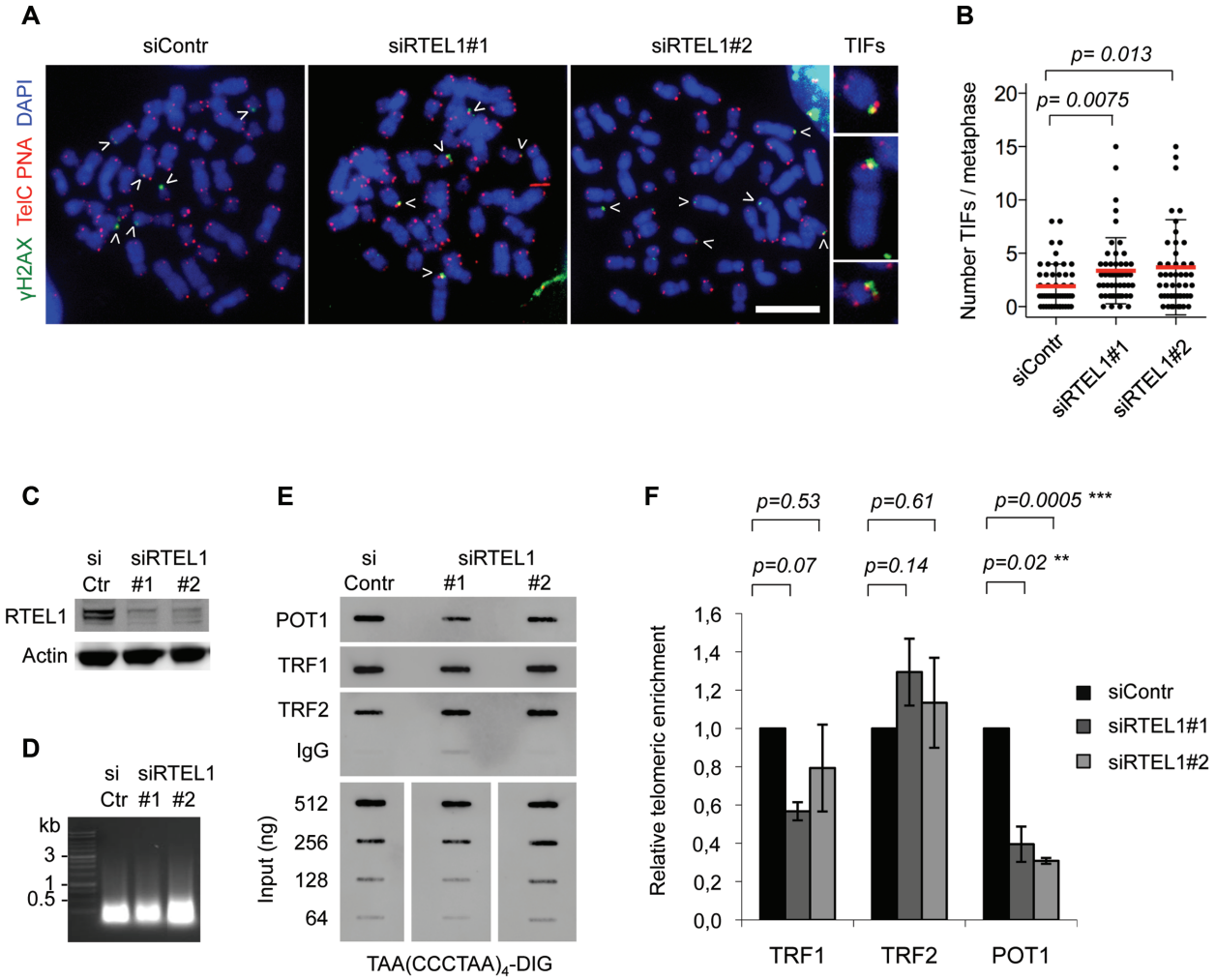

Figure 4. RTEL1 depletion induces limited telomere damage and decreases POT1 association with telomeres. (**A**) Representative images of HT1080-ST Meta-TIF analysis of cells treated with siControl, siRTEL1#1 and siRTEL1#2 using anti-γ-H2AX antibody (green) and TelC PNA probe (Cy3, red). Arrowheads, γ-H2AX signal at telomeres. Scale bar, 10 μm. Selected TIFs from siRTEL1#1 image are enlarged. (**B**) Quantification of A. Number of telomere dysfunction-induced foci (TIFs) per metaphase is shown. The mean values ($n = 30$ metaphases) ± SD are indicated. *P*-values, two-tailed student *t*-test. (**C**) ChIP experiments: western blot showing downregulation of RTEL1 in HT1080-ST using two specific siRNAs, siRTEL1#1 and #2. Actin was used as a loading control. (**D**) Sonication efficiency for the chromatin preparations. The 1 kb DNA ladder (Promega). (**E**) ChIP analysis of telomeric DNA upon downregulation of RTEL1 shows reduced levels of POT1 at telomeres while TRF1 and TRF2 levels were unchanged. The blot was revealed with a DIG-Tel-C-rich probe. Serial dilutions of input chromatin used for normalization are also shown. (**F**) Quantification of E. ChIP signals were normalized to DNA input and siControl. Data are represented as mean ($n = 3$–7) ± SEM. *P*-values, two-tailed student *t*-test. The amount of POT1 at telomeres following depletion of RTEL1 is significantly reduced.

the telomeric activities of human RTEL1 and in particular the regulation of telomere length homeostasis, have remained largely unexplored in experimental settings. In this study, we have investigated the role of human RTEL1 in different types of human cells. We have observed that transient depletion of RTEL1 is able to induce rapid (albeit limited) telomere shortening in telomerase-positive cell lines that carry both long telomeres and high levels of telomerase, such as TCL1301, HT1080-ST and U2OS-ST. On the other hand, RTEL1-dependent telomere shortening was not observed under the same experimental conditions in telomerase-negative primary fibroblasts (HCA2), or ALT-positive telomerase-negative osteo-sarcoma cell line (U2OS) nor in telomerase-positive cancer cell lines with relatively short telomeres, such as HT1080 and HeLa.

The fact that we did not detect telomere shortening in HT1080-ST cells simultaneously deleted for hTERT and depleted for RTEL1, indicate that the effect of RTEL1 on telomere length in these cells is telomerase dependent. This telomerase-dependent effect was not due to defects in telomerase biogenesis or to targeting to telomeres. Instead, RTEL1-deficient cells displayed a significant reduction of both G-overhang content and the amount of POT1 bound to telomeres. Strikingly, over-expression of POT1 in RTEL1-depleted cells was able to rescue the telomere shortening phenotype but not the overhang defect, thus revealing a hierarchy in the observed consequences following RTEL1 depletion, in which the loss of the overhang is the primary defect. We favor the interpretation that the diminution of POT1 at telomeres is secondary to the de-

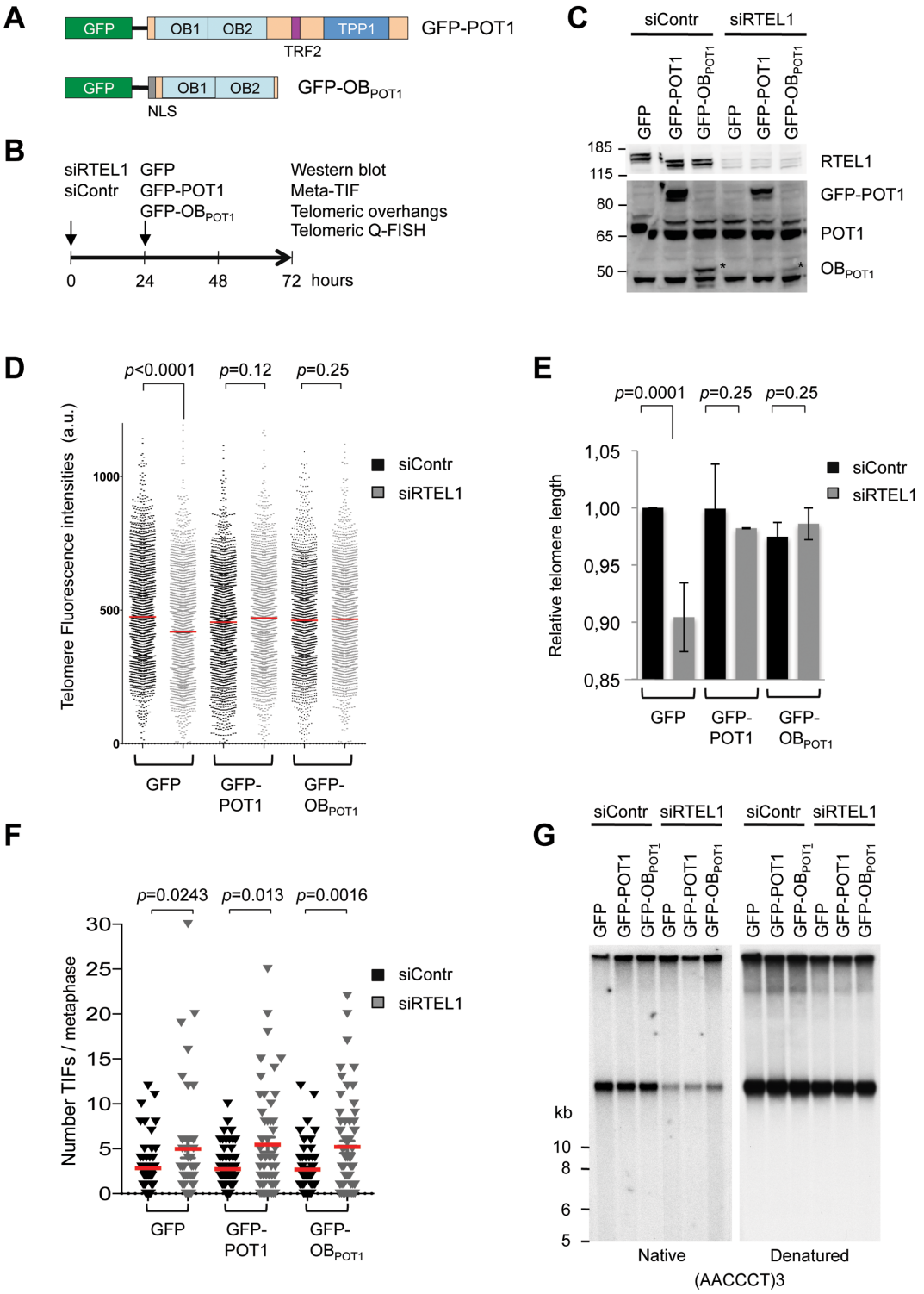

Figure 5. Overexpression of POT1 rescues the telomere length defect, but not the overhang defect, induced by RTEL1 depletion. (**A**) Constructs used for the expression of the full length POT1 and the two OB-fold domains of POT1 fused to GFP at the N-terminus. TRF2 and TPP1, respective binding sites for those proteins. NLS, nuclear localization signal. (**B**) Experimental outline. HT1080-ST cells were first transfected with siControl and siRTEL1, then after 24 h with GFP, GFP-POT1 and GFP-OB_{POT1} constructs prior to the collection of cells for the analyses of protein expression, telomere lengths, Meta-TIFs and telomeric overhangs. (**C**) Western blot showing downregulation of RTEL1 and expression of either GFP, GFP-POT1 or GFP-OB_{POT1} using anti-POT1 antibody. Molecular weight markers are indicated. (**D**) Representative quantification of telomere length analysis using Q-FISH. The graph represents telomere fluorescence intensities (a.u.) upon expression of GFP, GFP-POT1 and GFP-OB_{POT1} in HT1080-ST treated with siControl and siRTEL1. The mean values ($n = 30$ metaphases) are indicated. *P*-values, Wilcoxon rank-sum test. (**E**) Relative mean telomere length values from two independent Q-FISH experiments ± SEM. (**F**) Meta-TIF assay. TIFs associated with RTEL1 depletion are not suppressed by the expression of GFP-POT1 and GFP-OB_{POT1}. Mean values ($n = 50$ metaphases) are indicated. *P*-values, Wilcoxon rank-sum test. (**G**) In-gel hybridization under native condition using a radioactively labeled telomeric C-rich probe for detection of telomeric single stranded G-rich repeats using 6.5 μg of digested genomic DNA. After denaturation, the gel was re-hybridized using the same probe to detect the total amount of telomeric G-rich repeats.

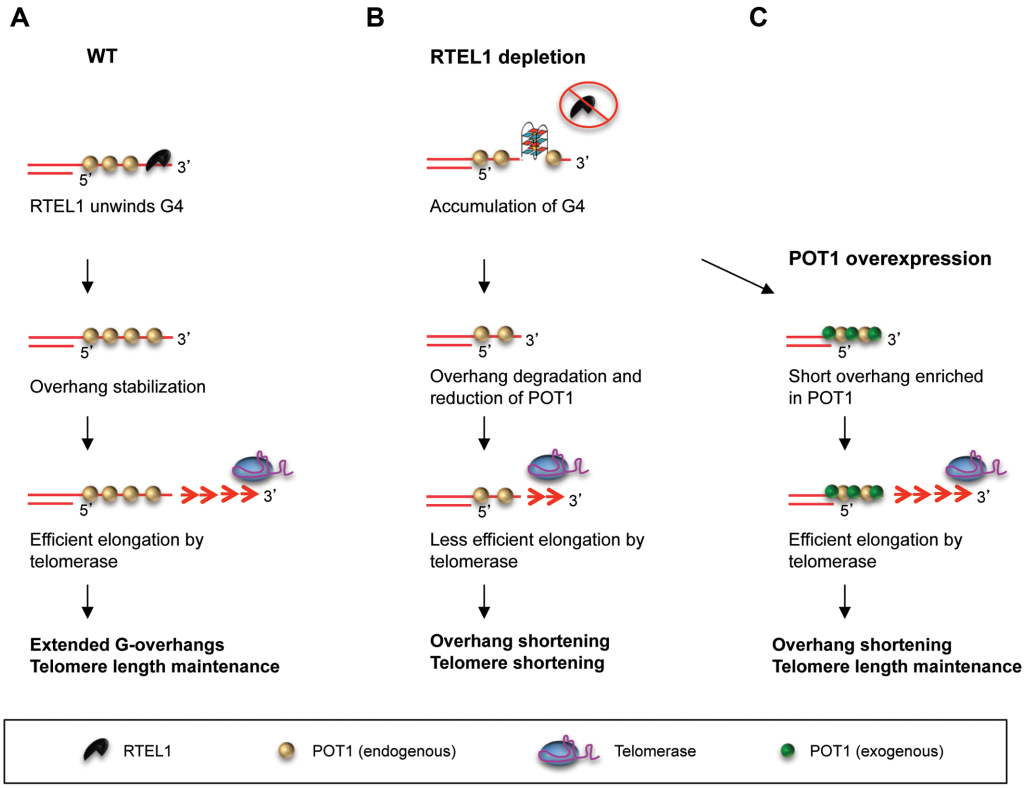

Figure 6. Model for RTEL1 regulation of telomere length homeostasis. (**A**) In human telomerase-positive cells with long telomeres and high telomerase activity, RTEL1 is required to stabilize the G-overhang, thus promoting POT1 binding, which stimulates telomerase activity. As a result, telomeres are overelongated. (**B**) In the absence of RTEL1, the G-overhang is trimmed, perhaps because the formation of secondary structures and the relative concentration of bound POT1 decreases, thus limiting the elongation by telomerase, despite normal accumulation of telomerase at telomeres. (**C**) In the absence of RTEL1, when an excess of POT1 is available, telomere length is restored likely through improved telomerase activity. However, since overhang protection depends on RTEL1, G-overhangs remain short.

crease in the amount of its main target sequence although another mechanism cannot at present be totally excluded. Interestingly, the fact that the amount of G-rich signal is not rescued by POT1 overexpression experiments suggests that the POT1 positive effect on telomerase activity (37) does not require long G-overhangs and that long G-overhangs are not absolutely required for POT1-mediated telomerase-dependent over-elongation. Instead, the accumulation of long G-overhangs in contexts where telomerase is active and telomeres are over-elongated requires RTEL1. While an interaction of RTEL1 with TRF2 has been observed (19), we failed to show any physical interaction between RTEL1 and POT1 (unpublished results).

Based on these results, we propose a model according to which RTEL1 is required, perhaps through its helicase activity to unwind secondary structures (11,12), to preserve the integrity of an extended telomeric G-overhang in cells with long telomeres and high telomerase activity (Figure 6A–C). The integrity of an extended overhang allows multiple molecules of POT1 to bind, perhaps promoting in this way a better presentation of the 3′ substrate to telomerase (38), which then can efficiently elongate telomeres (37). Under conditions in which RTEL1 is limiting, the extended overhangs may adopt secondary structures, possibly triggering degradation/cleavage activities, which in turn lead to a reduction of both G-overhang content and bound POT1. The combination of POT1 relative depletion and short 3′overhangs may then prevent telomerase from efficiently working on its substrate.

In human patient cells with mutated *RTEL1* telomere fragility and telomere loss are readily detected, suggesting that RTEL1 may impact telomeres differently in different cellular contexts. In agreement with this interpretation is the fact that while the absence of *Rtel1* in MEFs provokes a rapid and dramatic loss of telomere repeats as a consequence of severe abnormalities in telomere replication and rampant T-loop excision (12), deletion of *Rtel1* in mouse ESCs does not lead to T-loop excision and telomeres are set and maintained at a shortened length, thus suggesting that at least part of the Rtel1 effects in mouse cells on telomeres is telomerase dependent (9,10). Interestingly, a recent study shows that knocking out *Rtel1* in mouse somatic cells leads to a persistent and deleterious association of telomerase with 3′ substrates, seemingly created by reversed forks (39). In that model, suppression of telomerase rescues the telomere instability (telomere fragility and telomere loss), thus demonstrating the telomerase-dependent origin of RTEL1-related phenotypes. Contrary to this model, and in spite of an increased association of telomerase with telomeres in HT1080-ST cells depleted for RTEL1, we do not observe telomere fragility or sudden telomere loss. A comparison between different published studies is given in Supplemen-

tary Table S2. In addition to context-related dissimilarities, differences between studies may also reflect true differences in the way different types of cells deal with obstacles during replication fork progression. Whatever the case, all studies suggest that RTEL1 telomeric functions are exerted in the context of high telomerase activity and long telomeres.

In addition to these differences between experimental models, T-loop excision has not been observed in most HHS patients-derived cells examined (15,40). Instead, a diminished telomeric G-overhang has been documented in many RTEL1 HHS patients (18,41). Although in our study RTEL1-related phenotypes were restricted to human telomerase+ cancer cells with long telomeres, we cannot formally exclude that much subtler manifestations (remaining undetectable by the techniques used here) are associated with RTEL1 depletion in human cells with shorter telomeres and that these manifestations will become detectable in the long term. However, RTEL1 is an essential gene (thus precluding amplification of CRISPR/cas9 RTEL1-deleted clones) and our attempts to knockdown RTEL1 in a stable way using shRNA approaches have failed. It is possible that RTEL1 hypomorphic alleles may allow gradual accumulation of telomeric phenotypes over time. Alternatively, different molecular requirements may exist in the maintenance of very long telomeres. Indeed, it has been demonstrated that the mechanisms of telomere length homeostasis that act in cells with relatively short telomeres are subverted in cells with elongated telomeres (21,42,43).

In conclusion, we propose that RTEL1 promotes the telomerase-dependent over-elongation of 3′ overhangs in cells with already long telomeres by stabilizing the G-overhang/POT1 interaction. Physiological counterparts of this situation might be found during human embryonic development, thus ensuring efficient telomerase elongation and full telomere replenishment during a period of extreme cellular proliferation. Lack of functional RTEL1 will lead to precocious telomere shortening, thus contributing, together with defects in RTEL1 extratelomeric functions (13,30), to the severity of the clinical manifestations of HHS patients at birth.

SUPPLEMENTARY DATA

Supplementary Data are available at NAR Online.

ACKNOWLEDGEMENTS

We thank Mylène Perderiset for the RTEL1 antibody and Maria Emilia Lombardi Puig for the help with statistical analyses. The authors greatly acknowledge the Institut Curie PICT-IBiSA Imaging Facility and the Flow Cytometry Core Facility.

Author contributions: R.M.P., G.G., A.A., M.I.F.M., A.G., C.D., C.N. and I.D. performed experiments. S.B.C. and T.B.C. provided reagents. Y.T. and G.G. analyzed results. R.M.P., I.D. and A.L.V. analyzed results and wrote the paper.

FUNDING

Institut Curie and from Fondation ARC Fellowship (to R.M.P.); Agence Nationale pour la Recherche [ANR-14-CE10-0006-01 to A.L.V., in part]; Israel Science Foundation [1729/13 to Y.T.]; Israel Cancer Research Fund (to Y.T.); Worldwide Cancer Research [15-0338 to Y.T.]; Cancer Council NSW [RG 16-10 to T.M.B.]. Funding for open access charge: Institut Curie.

Conflict of interest statement. None declared.

REFERENCES

1. Makarov,V.L., Hirose,Y. and Langmore,J.P. (1997) Long G tails at both ends of human chromosomes suggest a C strand degradation mechanism for telomere shortening. *Cell*, **88**, 657–666.
2. McElligott,R. and Wellinger,R.J. (1997) The terminal DNA structure of mammalian chromosomes. *EMBO J.*, **16**, 3705–3714.
3. Palm,W. and de Lange,T. (2008) How shelterin protects mammalian telomeres. *Annu. Rev. Genet.*, **42**, 301–334.
4. Baumann,P. and Cech,T.R. (2001) Pot1, the putative telomere end-binding protein in fission yeast and humans. *Science*, **292**, 1171–1175.
5. Doksani,Y., Wu,J.Y., de Lange,T. and Zhuang,X. (2013) Super-resolution fluorescence imaging of telomeres reveals TRF2-dependent T-loop formation. *Cell*, **155**, 345–356.
6. Griffith,J.D., Comeau,L., Rosenfield,S., Stansel,R.M., Bianchi,A., Moss,H. and de Lange,T. (1999) Mammalian telomeres end in a large duplex loop. *Cell*, **97**, 503–514.
7. Shay,J.W. and Wright,W.E. (2005) Senescence and immortalization: role of telomeres and telomerase. *Carcinogenesis*, **26**, 867–874.
8. Blackburn,E.H. and Collins,K. (2011) Telomerase: an RNP enzyme synthesizes DNA. *Cold Spring Harb. Perspect. Biol.*, **3**, 1–10.
9. Ding,H., Schertzer,M., Wu,X., Gertsenstein,M., Selig,S., Kammori,M., Pourvali,R., Poon,S., Vulto,I., Chavez,E. *et al.* (2004) Regulation of murine telomere length by Rtel: an essential gene encoding a helicase-like protein. *Cell*, **117**, 873–886.
10. Uringa,E.J., Lisaingo,K., Pickett,H.A., Brind'Amour,J., Rohde,J.H., Zelensky,A., Essers,J. and Lansdorp,P.M. (2012) RTEL1 contributes to DNA replication and repair and telomere maintenance. *Mol. Biol. Cell*, **23**, 2782–2792.
11. Vannier,J.B., Sandhu,S., Petalcorin,M.I., Wu,X., Nabi,Z., Ding,H. and Boulton,S.J. (2013) RTEL1 is a replisome-associated helicase that promotes telomere and genome-wide replication. *Science*, **342**, 239–242.
12. Vannier,J.B., Pavicic-Kaltenbrunner,V., Petalcorin,M.I., Ding,H. and Boulton,S.J. (2012) RTEL1 dismantles T loops and counteracts telomeric G4-DNA to maintain telomere integrity. *Cell*, **149**, 795–806.
13. Ballew,B.J., Joseph,V., De,S., Sarek,G., Vannier,J.B., Stracker,T., Schrader,K.A., Small,T.N., O'Reilly,R., Manschreck,C. *et al.* (2013) A recessive founder mutation in regulator of telomere elongation helicase 1, RTEL1, underlies severe immunodeficiency and features of Hoyeraal Hreidarsson syndrome. *PLoS Genet.*, **9**, e1003695.
14. Ballew,B.J., Yeager,M., Jacobs,K., Giri,N., Boland,J., Burdett,L., Alter,B.P. and Savage,S.A. (2013) Germline mutations of regulator of telomere elongation helicase 1, RTEL1, in Dyskeratosis congenita. *Hum. Genet.*, **132**, 473–480.
15. Deng,Z., Glousker,G., Molczan,A., Fox,A.J., Lamm,N., Dheekollu,J., Weizman,O.E., Schertzer,M., Wang,Z., Vladimirova,O. *et al.* (2013) Inherited mutations in the helicase RTEL1 cause telomere dysfunction and Hoyeraal-Hreidarsson syndrome. *Proc. Natl. Acad. Sci. U.S.A.*, **110**, E3408–E3416.
16. Le Guen,T., Jullien,L., Touzot,F., Schertzer,M., Gaillard,L., Perderiset,M., Carpentier,W., Nitschke,P., Picard,C., Couillault,G. *et al.* (2013) Human RTEL1 deficiency causes Hoyeraal-Hreidarsson syndrome with short telomeres and genome instability. *Hum. Mol. Genet.*, **22**, 3239–3249.
17. Walne,A.J., Vulliamy,T., Kirwan,M., Plagnol,V. and Dokal,I. (2013) Constitutional mutations in RTEL1 cause severe dyskeratosis congenita. *Am. J. Hum. Genet.*, **92**, 448–453.
18. Lamm,N., Ordan,E., Shponkin,R., Richler,C., Aker,M. and Tzfati,Y. (2009) Diminished telomeric 3′ overhangs are associated with telomere dysfunction in Hoyeraal-Hreidarsson syndrome. *PLoS One*, **4**, e5666.

19. Sarek,G., Vannier,J.B., Panier,S., Petrini,J.H. and Boulton,S.J. (2015) TRF2 recruits RTEL1 to telomeres in S phase to promote t-loop unwinding. *Mol. Cell*, **57**, 622–635.
20. Gorbunova,V., Seluanov,A. and Pereira-Smith,O.M. (2003) Evidence that high telomerase activity may induce a senescent-like growth arrest in human fibroblasts. *J. Biol. Chem.*, **278**, 7692–7698.
21. Cristofari,G. and Lingner,J. (2006) Telomere length homeostasis requires that telomerase levels are limiting. *EMBO J.*, **25**, 565–574.
22. Arnoult,N., Saintome,C., Ourliac-Garnier,I., Riou,J.F. and Londono-Vallejo,A. (2009) Human POT1 is required for efficient telomere C-rich strand replication in the absence of WRN. *Genes Dev.*, **23**, 2915–2924.
23. Arnoult,N., Shin-Ya,K. and Londono-Vallejo,J.A. (2008) Studying telomere replication by Q-CO-FISH: the effect of telomestatin, a potent G-quadruplex ligand. *Cytogenet. Genome Res.*, **122**, 229–236.
24. Ourliac-Garnier,I. and Londono-Vallejo,A. (2011) Telomere length analysis by quantitative fluorescent in situ hybridization (Q-FISH). *Methods Mol. Biol.*, **735**, 21–31.
25. Kim,N.W., Piatyszek,M.A., Prowse,K.R., Harley,C.B., West,M.D., Ho,P.L., Coviello,G.M., Wright,W.E., Weinrich,S.L. and Shay,J.W. (1994) Specific association of human telomerase activity with immortal cells and cancer. *Science*, **266**, 2011–2015.
26. Cesare,A.J., Kaul,Z., Cohen,S.B., Napier,C.E., Pickett,H.A., Neumann,A.A. and Reddel,R.R. (2009) Spontaneous occurrence of telomeric DNA damage response in the absence of chromosome fusions. *Nat. Struct. Mol. Biol.*, **16**, 1244–1251.
27. Hemann,M.T. and Greider,C.W. (1999) G-strand overhangs on telomeres in telomerase-deficient mouse cells. *Nucleic Acids Res.*, **27**, 3964–3969.
28. Londono-Vallejo,J.A., Der-Sarkissian,H., Cazes,L., Bacchetti,S. and Reddel,R.R. (2004) Alternative lengthening of telomeres is characterized by high rates of telomeric exchange. *Cancer Res.*, **64**, 2324–2327.
29. Henson,J.D., Cao,Y., Huschtscha,L.I., Chang,A.C., Au,A.Y., Pickett,H.A. and Reddel,R.R. (2009) DNA C-circles are specific and quantifiable markers of alternative-lengthening-of-telomeres activity. *Nat. Biotechnol.*, **27**, 1181–1185.
30. Schertzer,M., Jouravleva,K., Perderiset,M., Dingli,F., Loew,D., Le Guen,T., Bardoni,B., de Villartay,J.P., Revy,P. and Londono-Vallejo,A. (2015) Human regulator of telomere elongation helicase 1 (RTEL1) is required for the nuclear and cytoplasmic trafficking of pre-U2 RNA. *Nucleic Acids Res.*, **43**, 1834–1847.
31. Egan,E.D. and Collins,K. (2012) Biogenesis of telomerase ribonucleoproteins. *RNA*, **18**, 1747–1759.
32. Cohen,S.B. and Reddel,R.R. (2008) A sensitive direct human telomerase activity assay. *Nat. Methods*, **5**, 355–360.
33. Stern,J.L., Zyner,K.G., Pickett,H.A., Cohen,S.B. and Bryan,T.M. (2012) Telomerase recruitment requires both TCAB1 and Cajal bodies independently. *Mol. Cell. Biol.*, **32**, 2384–2395.
34. Pascolo,E., Wenz,C., Lingner,J., Hauel,N., Priepke,H., Kauffmann,I., Garin-Chesa,P., Rettig,W.J., Damm,K. and Schnapp,A. (2002) Mechanism of human telomerase inhibition by BIBR1532, a synthetic, non-nucleosidic drug candidate. *J. Biol. Chem.*, **277**, 15566–15572.
35. Celli,G.B. and de Lange,T. (2005) DNA processing is not required for ATM-mediated telomere damage response after TRF2 deletion. *Nat. Cell Biol.*, **7**, 712–718.
36. Zhu,X.D., Niedernhofer,L., Kuster,B., Mann,M., Hoeijmakers,J.H. and de Lange,T. (2003) ERCC1/XPF removes the 3′ overhang from uncapped telomeres and represses formation of telomeric DNA-containing double minute chromosomes. *Mol. Cell*, **12**, 1489–1498.
37. Colgin,L.M., Baran,K., Baumann,P., Cech,T.R. and Reddel,R.R. (2003) Human POT1 facilitates telomere elongation by telomerase. *Curr. Biol.*, **13**, 942–946.
38. Zaug,A.J., Podell,E.R. and Cech,T.R. (2005) Human POT1 disrupts telomeric G-quadruplexes allowing telomerase extension in vitro. *Proc. Natl. Acad. Sci. U.S.A.*, **102**, 10864–10869.
39. Margalef,P., Kotsantis,P., Borel,V., Bellelli,R., Panier,S. and Boulton,S.J. (2018) Stabilization of reversed replication forks by telomerase drives telomere catastrophe. *Cell*, **172**, 439–453.
40. Speckmann,C., Sahoo,S.S., Rizzi,M., Hirabayashi,S., Karow,A., Serwas,N.K., Hoemberg,M., Damatova,N., Schindler,D., Vannier,J.B. *et al.* (2017) Clinical and molecular heterogeneity of RTEL1 deficiency. *Front. Immunol.*, **8**, 1–19.
41. Marsh,J.C.W., Gutierrez-Rodrigues,F., Cooper,J., Jiang,J., Gandhi,S., Kajigaya,S., Feng,X., Ibanez,M., Donaires,F.S., Lopes da Silva,J.P. *et al.* (2018) Heterozygous RTEL1 variants in bone marrow failure and myeloid neoplasms. *Blood Adv.*, **2**, 36–48.
42. Pickett,H.A., Cesare,A.J., Johnston,R.L., Neumann,A.A. and Reddel,R.R. (2009) Control of telomere length by a trimming mechanism that involves generation of t-circles. *EMBO J.*, **28**, 799–809.
43. Pickett,H.A., Henson,J.D., Au,A.Y., Neumann,A.A. and Reddel,R.R. (2011) Normal mammalian cells negatively regulate telomere length by telomere trimming. *Hum. Mol. Genet.*, **20**, 4684–4692.